# Chapter 13

# Toward Understanding Black Hole Merger Dynamics

The stunning breakthroughs in Numerical Relativity over the past few years, starting with those by Pretorius [155] in spring 2005, have provided greater insight into the realm of strongly curved spacetime and dynamical gravity. Non-spinning binary black hole merger simulations are quickly becoming the norm, and numerical relativists have started looking at more interesting situations, including the orbit and merger of spinning binary black holes. Surprising results from this sort of situation are exemplified in the *extreme-kick configuration* in which two identical, spinning black holes are initially in a (quasi-)circular orbit, with oppositely directed spins lying in the orbital plane (figure 13.1).

As Campanelli, Lousto, Zlochower, and Merritt [156, 157] (CLZM) discovered and Healy et al. [158] helped flesh out, of all equal mass, quasi-circular initial configurations, this one has the

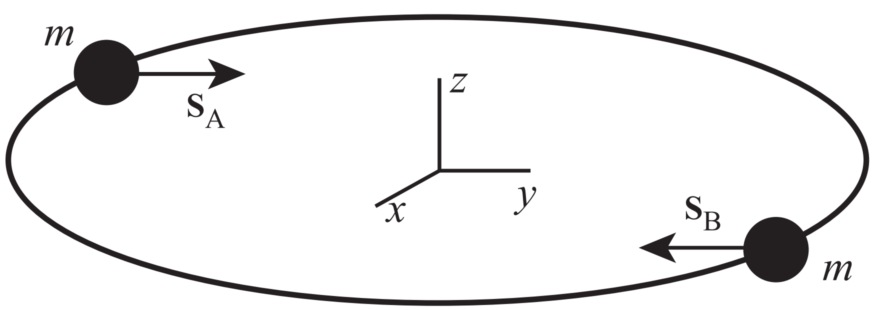


Figure 13.1: Extreme-kick Configuration
Extreme-kick configuration for a black-hole binary: Identical holes, $A$ and $B$ with masses $m = M/2$ move in a circular orbit with their spin angular momenta $\boldsymbol{S}_A$ and $\boldsymbol{S}_B$ antialigned and lying in the orbital plane.

largest kick speed for the final black hole. Not only that, it also exhibits intriguing orbital motions.

During the inspiral phase, as the holes circle each other, they bob up and down (in the $z$ direction of figure 13.1), sinusoidally and synchronously. After merger the combined hole gets kicked up or down with a final speed that depends on the orbital phase at merger (relative to the spin directions). This bobbing-then-kick, as deduced by CLZM from numerical simulations, is graphed quantitatively in figure 13.2.

Qualitatively, Pretorius [159] has offered a lovely physical explanation for the holes' bobbing (figure 13.2) in this configuration: In figure 13.3, taken from his paper, we see snapshots of the holes at four phases in their orbital motion. In each snapshot, each hole's spin drags space into motion (drags inertial frames) in the direction depicted by gray, semicircular arrows. In phase B, hole 1 drags space and thence hole 2 into the sheet of paper (or computer screen); and hole 2 drags space and thence hole 1 also inward. In phase D each hole drags the other outward. This picture agrees in phasing and semiquantitatively in amplitude with the bobbing observed in the simulations (figure 13.2).

However, momentum conservation dictates that, when the holes are moving upward together with momentum $p^z_A + p^z_B$, there must be some equal and opposite downward momentum in their gravitational field (in the curved spacetime surrounding them); and when the holes are moving downward, there must be an equal and opposite upward field momentum. Our aim is to quantitatively answer the following questions: How is this field momentum distributed? What are the details of the momentum flow between field and holes? And to what extent are other momentum-flow processes responsible for the motion shown in figure 13.2?

The outline of this chapter is as follows: section 13.1 gives a brief overview of the Landau-Lifshitz formalism, which can be used to calculate the energy and momentum content of the gravitational field, section 13.2 sets up the calculation of momentum consveration by splitting the total momentum into its respective pieces, section 13.3 calculates each of the pieces of the momentum both for the general binary and in the extreme-kick configuration, and section 13.4 combines these results to show that the momentum of the objects balanced by the field momentum.

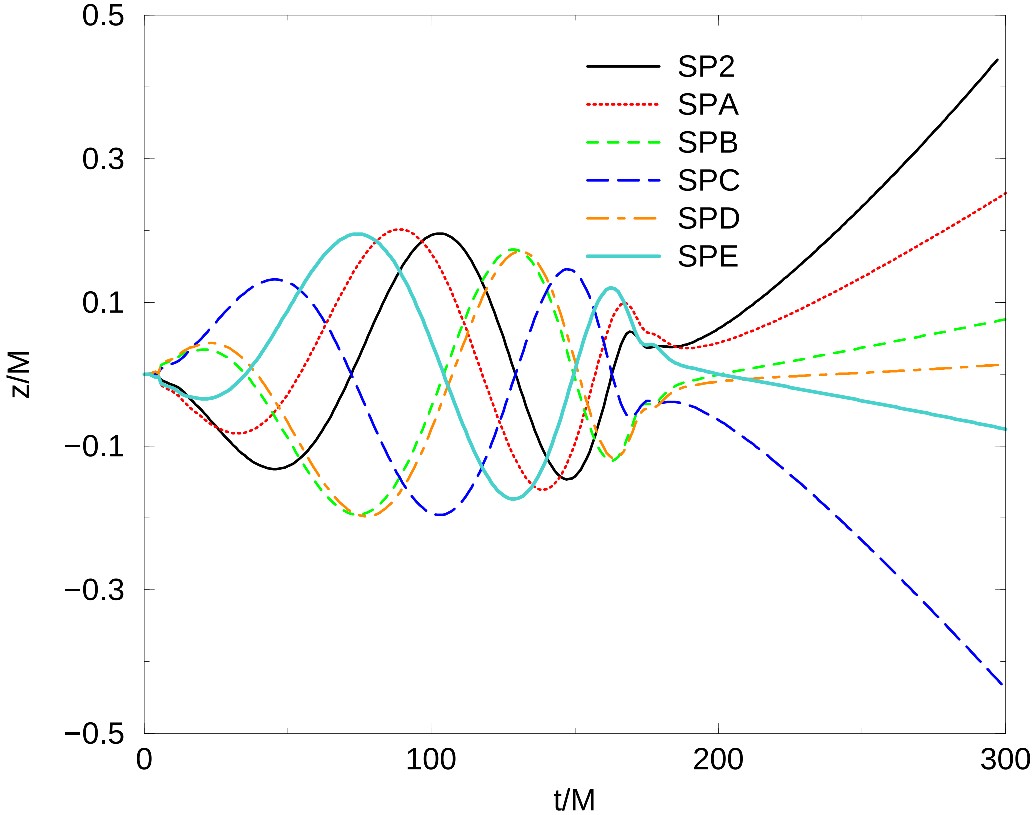


Figure 13.2: Bobbing Motion in Extreme-kick Configuration
Bobbing and kick of binary black holes in the extreme-kick configuration of figure 13.1, as simulated by Campanelli, Lousto, Zlochower, and Merritt (CLZM) [157]. Plotted vertically (as a function of time horizontally) is the identical height $z$ of the two black holes, and then transitioning through merger (presumably at $t/M \sim 170$), the height of the merged hole, above the initial orbital plane. This height versus time is shown for six different initial configurations, each leading to a different orbital phase at merger. In all six configurations, the initial holes' spins are half the maximum allowed, $a/m = 0.5$. The height $z$ and time $t$ are those of the "punctures" that represent the holes' centers in the CLZM computations, as defined in their computational coordinate system, which becomes Lorentz at large radii. These $z$ and $t$ are measured in units of the system's total mass $M \simeq 2m$.

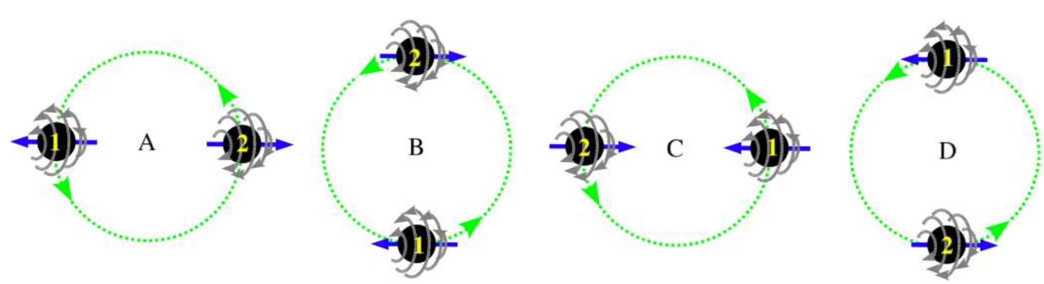


Figure 13.3: Pretorius' Explanation
Pretorius' physical explanation for the holes' bobbing in the extreme-kick configuration, in which the effect is attributed qualitatively to frame-dragging.

## 13.1 The Landau-Lifshitz Formalism in Brief

Here we give a detailed analysis of momentum flow in generic compact binary systems. We begin in this section with a brief review of the Landau-Lifshitz (LL) formulation of general relativity as a nonlinear field theory in flat spacetime [160].

The Landau-Lifshitz formulation [160] starts by choosing an arbitrary coordinate system that is asymptotically Lorentz, to this an auxiliary flat spacetime is added by asserting that the chosen ("preferred") coordinates are globally Lorentz in the auxiliary spacetime (so in them the auxiliary metric has components diag$(-1, 1, 1, 1)$). In this formulation, gravity is described by the physical metric density

$$\mathfrak{g}^{\mu\nu} = \sqrt{-g}g^{\mu\nu} \ , \tag{13.1}$$

where $g$ is the determinant of the covariant components of the physical metric, and $g^{\mu\nu}$ are the contravariant components of the physical metric.

The EFEs are then reformulated as a nonlinear field theory in the space of the flat, auxiliary metric. Making use of the superpotential

$$H^{\mu\alpha\nu\beta} \equiv \mathfrak{g}^{\mu\nu}\mathfrak{g}^{\alpha\beta} - \mathfrak{g}^{\mu\alpha}\mathfrak{g}^{\nu\beta} \ , \tag{13.2}$$

the EFEs are given by

$$H^{\mu\alpha\nu\beta}{}_{,\alpha\beta} = 16\pi\tau^{\mu\nu} \ , \tag{13.3}$$

where $\tau^{\mu\nu} = (-g)(T^{\mu\nu} + t^{\mu\nu}_{\mathrm{LL}})$ is the total effective stress-energy tensor, indices after the comma denote partial derivatives (covariant derivatives with respect to the flat auxiliary metric), and the Landau-Lifshitz pseudotensor $t^{\mu\nu}_{\mathrm{LL}}$ (actually a real tensor in the auxiliary flat spacetime) is given by equation (100.7) of LL [160] or equivalently equation (20.22) of MTW [1]. By virtue of the symmetries of the superpotential (which are the same as those of the Riemann tensor), the field equations in the form (13.3) imply the differential conservation law for 4-momentum

$$\tau^{\mu\nu}{}_{,\nu} = 0 \ , \tag{13.4}$$

which is equivalent to $T^{\mu\nu}{}_{;\nu} = 0$ (where the semicolon denotes a covariant derivative with respect to the physical metric).

It is shown in LL and in MTW that the total 4-momentum of any isolated system (as measured gravitationally in the asymptotically flat region far from the system) is

$$p^{\mu}_{\rm tot} = \frac{1}{16\pi} \oint_{\mathcal{S}} H^{\mu\alpha 0 j}{}_{,\alpha} d\Sigma_j \ , \tag{13.5}$$

where $d\Sigma_j$ is the surface-area element defined using the flat auxiliary metric, and the integral is over an arbitrarily large closed surface $\mathcal{S}$ surrounding the system. Differentiating this, we find

$$\frac{dp^{\mu}_{\rm tot}}{dt} = \frac{1}{16\pi} \oint_{\mathcal{S}} H^{\mu\alpha 0 j}{}_{,\alpha 0} d\Sigma_j \ . \tag{13.6}$$

Let us look at $H^{\mu\alpha 0 j}{}_{,\alpha 0} = H^{\mu\alpha\nu j}{}_{,\alpha\nu} - H^{\mu\alpha k j}{}_{,\alpha k}$. The first term is $-16\pi\tau^{\mu j}$ by virtue of the field equations (13.3) and the antisymmetry of the superpotential on its last two indices (13.2). That same antisymmetry on the second term $-H^{\mu\alpha k j}{}_{,\alpha k}$ permits us to write it as the curl of a 3-vector field, whose surface integral vanishes by virtue of Stokes' theorem. Combining these two results we find the total 4-momentum satisfies the standard conservation law

$$\frac{dp^{\mu}_{\rm tot}}{dt} = -\oint_{\mathcal{S}} \tau^{\mu j} d\Sigma_j \ . \tag{13.7}$$

This proof has also been given in LL and MTW where it relied on an assumption that the interior of $\mathcal{S}$ be simply connected, i.e., that it not contain any black holes.

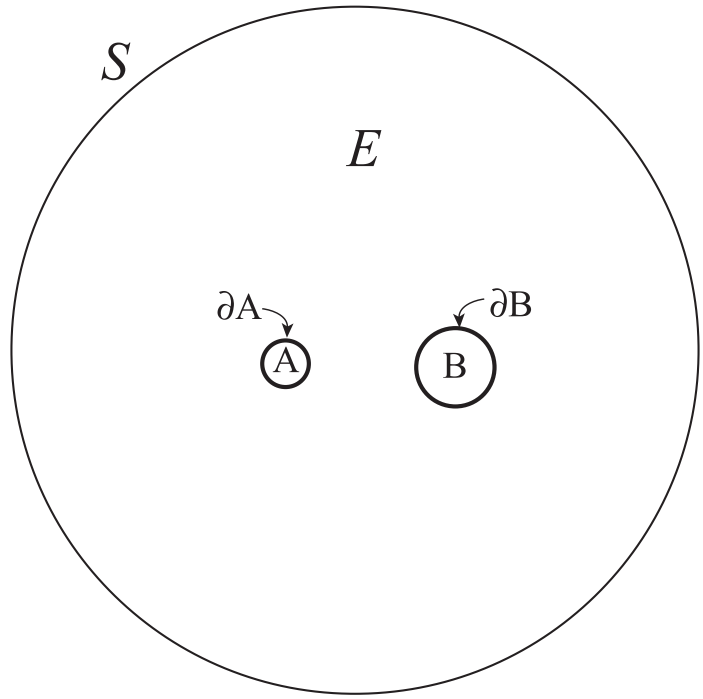


Figure 13.4: Division of Space
The regions of space around and inside a compact binary system.

## 13.2 Momentum Conservation for a Fully Nonlinear Compact Binary

We now apply this LL formalism to a binary system made of black holes and/or neutron stars; see figure 13.4. We denote the binary's two bodies by the letters $A$ and $B$, and the regions of space inside them by these same letters, and their surfaces by $\partial A$ and $\partial B$. For a black hole, $\partial A$ could be the hole's absolute event horizon or its apparent horizon, whichever one wishes. For a neutron star, $\partial A$ will be the star's physical surface. We denote by $\mathcal{E}$ the region outside both bodies, but inside the arbitrarily large surface $\mathcal{S}$ where the system's total momentum is computed.

By applying Gauss's theorem to equation (13.5) for the binary's total 4-momentum and using the EFE (13.3), we obtain an expression for the binary's total 4-momentum as a sum over contributions from each of the bodies and from the gravitational field in the region $\mathcal{E}$ outside them:

$$p^{\mu}_{\rm tot} = p^{\mu}_{A} + p^{\mu}_{B} + p^{\mu}_{\rm field} \, . \qquad (13.8a)$$

Here

$$p^\mu_A \equiv \frac{1}{16\pi}\oint_{\partial A} H^{\mu\alpha 0j}{}_{,\alpha} d\Sigma_j \tag{13.8b}$$

is the 4-momentum of body $A$ and similarly for body $B$, and

$$p^\mu_{\rm field} \equiv \int_{\mathcal{E}} \tau^{0\mu} d^3x \tag{13.8c}$$

is the gravitational field's 4-momentum in the surrounding space.

If either of the bodies has a simply connected interior (is a star rather than a black hole), then we can use Gauss's theorem and the EFEs (13.3) to convert the surface integral (13.8b) for the body's 4-momentum into a volume integral over the body's interior:

$$p^\mu_A = \int_A \tau^{0\mu} d^3x \ . \tag{13.8d}$$

By an obvious extension of the argument we used to derive equation (13.7) for the rate of change of the binary's total 4-momentum, we can deduce from equation (13.8b) the corresponding equation for the rate of change of the 4-momentum of body $A$:

$$\frac{dp^\mu_A}{dt} = -\oint_{\partial A} (\tau^{\mu k} - \tau^{\mu 0} v^k_A) d\Sigma_k \ . \tag{13.9}$$

Here the second term arises from the motion of the boundary of body $A$ with coordinate velocity $v^k_A = dx^k_{A\ \rm cm}/dt$. Equation (13.9) describes the flow of field 4-momentum into and out of body $A$.

We shall use equations (13.8), (13.7), and (13.9), specialized to linear momentum (index $\mu$ made spatial) as foundations for our study of momentum flow in compact binaries.

The actual values of the body and field 4-momenta, computed in the above ways, will depend on the arbitrary coordinate system that we chose, in which to make the auxiliary metric be diag$(-1, 1, 1, 1)$ and in which to perform the above computations. This is a "gauge dependence," which we will fix by our choice of coordinates. In the remainder of this chapter we shall choose

Harmonic coordinates, so the gravitational field satisfies the Harmonic gauge condition

$$\mathfrak{g}^{\alpha\beta}{}_{,\beta} = 0 \, , \tag{13.10}$$

and we shall specialize the above equations to the 1.5 post-Newtonian approximation and use them to study momentum flow during the inspiral phase of generic compact binaries.

## 13.3 Post-Newtonian Momentum Flow in Generic Compact Binaries

### 13.3.1 Field Momentum Outside the Bodies

In Harmonic gauge at leading post-Newtonian order, the Landau-Lifshitz formalism gives for the density of field momentum

$$\tau^{0j}\boldsymbol{e}_j = -\frac{\boldsymbol{g}\times\boldsymbol{H}}{4\pi} + \frac{3}{4\pi}\dot{U}_N\boldsymbol{g} \tag{13.11}$$

(equation (4.1a) of [161]). Here, to the accuracy we need, $\boldsymbol{g}$ is the Newtonian gravitational acceleration field (the *gravitoelectric field*), $\boldsymbol{H}$ is the gravitational analog of the magnetic field (the *gravitomagnetic field*), $U_N$ is the Newtonian potential and the dot denotes differentiation with respect to time, and $\boldsymbol{e}_j$ is the $j$th basis vector of the flat-spacetime field theory that we are using.

This field momentum can be split into several pieces, only one of which will flow back and forth between the field and the bobbing holes. Each of the components in equation (13.11) (i.e., $\boldsymbol{g}$, $\boldsymbol{H}$, and $U_N$) have contributions from body $A$ and body $B$, where

$$\boldsymbol{g}_A = -\frac{m}{r_A^2}\boldsymbol{n}_A \, , \tag{13.12a}$$

$$U_{N,A} = \frac{m}{r_A} \, , \tag{13.12b}$$

(equations (2.5) and (6.1) of [161]). In addition, $\boldsymbol{H}$ can be split into terms arising from either velocity ($\boldsymbol{H}^{\rm velo}$) or spin ($\boldsymbol{H}^{\rm spin}$) contributions of a particular body:

$$\boldsymbol{H}_A^{\rm velo} = \frac{4m_A(\boldsymbol{n}_A \times \boldsymbol{v}_A)}{r_A^2}\,, \tag{13.12c}$$

$$\boldsymbol{H}_A^{\rm spin} = -2\frac{(3\boldsymbol{n}_A \cdot \boldsymbol{S}_A)\boldsymbol{n}_A - \boldsymbol{S}_A}{r_A^3}\,, \tag{13.12d}$$

(equations (2.5) and (6.1) of [161]), with $\boldsymbol{n}_A$ the unit radial vector pointing from the center of body $A$ to the field point, $r_A$ the distance from the center of body $A$ to the field point, $\boldsymbol{v}_A$ the vectorial velocity of body $A$, and $\boldsymbol{S}_A$ the vectorial angular momentum of body $A$. The fields for body $B$ are the same as equations (13.12), but with each subscript $A$ replaced by a $B$.

The full field momentum density is written most concisely as

$$\tau^{0j} = \tau^{0j}_{\rm spin} + \tau^{0j}_{\rm velo}, \tag{13.13a}$$

where $\tau^{0j}_{\rm spin}$ and $\tau^{0j}_{\rm velo}$ are the terms that depend on the spins and the velocities, respectively. These terms are given by

$$\begin{aligned}\tau^{0j}_{\rm spin}\boldsymbol{e}_j &= \frac{m_B}{2\pi r_A^3 r_B^2}\left[3(\boldsymbol{S}_A \cdot \boldsymbol{n}_A)(\boldsymbol{n}_A \times \boldsymbol{n}_B) - (\boldsymbol{S}_A \times \boldsymbol{n}_B)\right] \\ &\quad -\frac{1}{2\pi}\frac{m_A}{r_A^5}(\boldsymbol{S}_A \times \boldsymbol{n}_A) + (A \leftrightarrow B),\end{aligned} \tag{13.13b}$$

and

$$\begin{aligned}\tau^{j0}_{\rm velo}\boldsymbol{e}_j &= \frac{m_A}{4\pi r_A^2}\left\{\frac{m_B[4(\boldsymbol{n}_B \cdot \boldsymbol{v}_A)\boldsymbol{n}_A - 4(\boldsymbol{n}_A \cdot \boldsymbol{n}_B)\boldsymbol{v}_A]}{r_B^2}\right. \\ &\quad \left. -\frac{3m_B(\boldsymbol{n}_A \cdot \boldsymbol{v}_A)\boldsymbol{n}_B}{r_B^2} + \frac{m_A[(\boldsymbol{n}_A \cdot \boldsymbol{v}_A)\boldsymbol{n}_A - 4\boldsymbol{v}_A]}{r_A^2}\right\} \\ &\quad +(A \leftrightarrow B),\end{aligned} \tag{13.13c}$$

where $(A \leftrightarrow B)$ means the same expression with labels $A$ and $B$ interchanged.

We are only interested in that portion of the field momentum that is induced by the holes' spins, since this is the portion that must flow back and forth between the field and the bobbing holes in order to conserve total momentum. As can be seen from equations (13.12), this portion arises from one hole's gravitoelectric field $\boldsymbol{g}$ coupling to the spin-induced part of the other hole's gravitomagnetic field $\boldsymbol{H}^{\rm spin}$

$$\delta\tau^{0j}\boldsymbol{e}_j = -\frac{\boldsymbol{g}_A \times \boldsymbol{H}_B^{\rm spin}}{4\pi} - \frac{\boldsymbol{g}_B \times \boldsymbol{H}_A^{\rm spin}}{4\pi} \ . \tag{13.14}$$

Combining equations (13.14) and (13.12) we obtain for the binary's density of field momentum (that portion which must flow during bobbing)

$$\delta\tau^{0j}\boldsymbol{e}_j = \frac{m_B}{2\pi r_A^3 r_B^2}\left[3(\boldsymbol{S}_A\cdot\boldsymbol{n}_A)(\boldsymbol{n}_A\times\boldsymbol{n}_B) - (\boldsymbol{S}_A\times\boldsymbol{n}_B)\right] + (A\leftrightarrow B) \ . \tag{13.15}$$

In order to integrate this over the region $\mathcal{E}$, we find it convenient to rewrite the bodies' gravitoelectric (13.12a) and gravitomagnetic fields (13.12d) as

$$g_K^j = m_K\left(\frac{1}{r_K}\right)_{,j} \ , \quad H_K^j = -2S_K^i\left(\frac{1}{r_K}\right)_{,ij} \ , \tag{13.16}$$

where $K$ is $A$ or $B$ and where, as before, $r_K$ is the (flat-space) distance of the field point from the center of mass of body $K$. Inserting equations (13.16) into expression (13.14) and manipulating the derivatives, we obtain the following expression for the field momentum density:

$$\delta\tau^{0j} = -\frac{1}{2\pi}\epsilon_{jpl}\left[S_A^q m_B\left(\frac{1}{r_A}\right)_{,q}\left(\frac{1}{r_B}\right)_{,l}\right]_{,p} + (A\leftrightarrow B) \ . \tag{13.17}$$

Notice that this expression for the momentum density is the curl of a vector field; or, equally well, it can be viewed as the divergence of a tensor field.

The total spin-induced, flowing field momentum is the integral of expression (13.17) over the exterior region $\mathcal{E}$ (cf., figure 13.4). Using Gauss's law, that volume integral can be converted into the following integral over the boundary of $\mathcal{E}$

$$\delta p^j_{\rm field} = -\frac{1}{2\pi}\epsilon_{jpl}S_A^q m_B\int_{\partial\mathcal{E}}\left(\frac{1}{r_A}\right)_{,q}\left(\frac{1}{r_B}\right)_{,l} d\Sigma_p + (A\leftrightarrow B) \ . \tag{13.18}$$

The boundary of $\mathcal{E}$ has three components: the surface $\mathcal{S}$ far from the binary on which we compute the binary's total momentum, and the surfaces $\partial A$ and $\partial B$ of bodies $A$ and $B$. The integral over $\mathcal{S}$ vanishes because the integrand is $\propto 1/r^4$ and the surface area is $\propto r^2$ and $\mathcal{S}$ is arbitrarily far from the binary, $r \to \infty$. When integrating over the bodies' surfaces, we shall flip the direction of the vectorial surface element so it points out of the bodies (into $\mathcal{E}$), thereby picking up a minus sign and bringing equation (13.18) into the form

$$\begin{aligned} \delta p^j_{\text{field}} &= \frac{1}{2\pi}\epsilon_{jpl} S^q_A m_B \left[\int_{\partial\mathcal{A}} \left(\frac{1}{r_A}\right)_{,q}\left(\frac{1}{r_B}\right)_{,l} d\Sigma_p \right. \\ &\left. + \int_{\partial\mathcal{B}} \left(\frac{1}{r_A}\right)_{,q}\left(\frac{1}{r_B}\right)_{,l} d\Sigma_p\right] + (A \leftrightarrow B)\,. \end{aligned} \tag{13.19}$$

We presume (as is required by the PN approximation) that the bodies' separation is large compared to their radii. Then on $\partial A$, we can write $(1/r_A)_{,q} = -n^q_A/r^2_A$ and $(1/r_B)_{,l} = n^l_{AB}/r^2_{AB}$, where $n_A$ is the unit vector pointing away from the center of mass of body $A$, $n^l_{AB}$ is the unit vector pointing from the center of mass of body $B$ toward the center of mass of body $A$, and $r_{AB}$ is the (flat-spacetime) distance between the two bodies' centers of mass. The first integral in equation (13.19) then becomes $n_{AB}/r^2_B \int_{\partial A} n^q_A/r^2_A d\Sigma_p$. For simplicity we take the surface of integration to be a sphere immediately above the physical surface of body $A$ and ignore the tiny contribution from the region between that sphere and the physical surface. On this sphere, we write $d\Sigma_p = r^2_A n^p_A d\Omega_A$, where $d\Omega_A$ is the solid angle element, and we then carry out the angular integral using the relation $\int_{\partial A} n^q_A n^p_A d\Omega_A = (4\pi/3)\delta_{qp}$. Thereby we obtain for the first integral in (13.19) $(4\pi/3)\delta_{qp} n_{AB}/r^2_B$ independent of the radius $r_A$ of the sphere of integration. (If the body is not spherical, the contribution from the tiny volume between our spherical integration surface and the physical surface will be negligible.) Evaluating the second integral in equation (13.19) in the same way, and carrying out straightforward manipulations, we obtain for the external field momentum

$$\delta \boldsymbol{p}_{\text{field}} = \frac{2}{3r^2_{AB}}(m_B \boldsymbol{S}_A - m_A \boldsymbol{S}_B) \times \boldsymbol{n}_{AB}\ . \tag{13.20}$$

#### 13.3.1.1 Field Momentum Specialized to the Extreme-Kick Configuration

For the extreme-kick configuration, which has $m_A = m_B = m$ and $\boldsymbol{S}_B = -\boldsymbol{S}_A$, the field momentum (13.20) becomes

$$\delta \boldsymbol{p}_{\rm field} = \frac{4}{3}\frac{m}{r_{AB}^2}\boldsymbol{S}_A \times \boldsymbol{n}_{AB} \ . \tag{13.21}$$

Figure 13.5 shows the $z$-component (perpendicular to the orbital plane) of the field-momentum density $\delta\tau^{0z}$, as measured in the orbital plane at four different moments in the binary's orbital evolution. Only that part of the momentum that flows during bobbing (equation (13.15)) is pictured. Red depicts momentum density flowing out of the paper ($+z$ direction), and blue, into the paper. The yellow arrows show the holes' vectorial spins $\boldsymbol{S}$, and the arrowed circle is the binary's orbital trajectory. In the top-left and bottom-right frames, the black holes are momentarily stationary at the top and bottom of their bobbing. Nevertheless, the momentum density has a nontrivial distribution. In the top-right and bottom-left frames, the black holes are moving downward and upward, respectively, with maximum speed. In both cases, the field-momentum density between the two holes flows in the same direction as the bobbing, whereas the momentum surrounding the binary is in the opposite direction and larger. This leads to net momentum conservation for the binary, as discussed in section 13.4.

It is worth noting that the four figures, going counterclockwise from the top-left, are taken a quarter period apart in orbital phase. The first and third differ by half an orbital period (as do the second and fourth); and, consequently, the momentum patterns of each pair are identical, but signs are reversed (red exchanged with blue, as dictated by the symmetry of the configuration). This feature is responsible for the sinusoidal bobbing.

### 13.3.2 Centers of Mass and Equation of Motion for the Binary's Compact Bodies

Restrict attention, temporarily, to a body that is a star rather than a black hole, and temporarily omit the subscript $K$ that identifies which body. Then, following the standard procedure in special

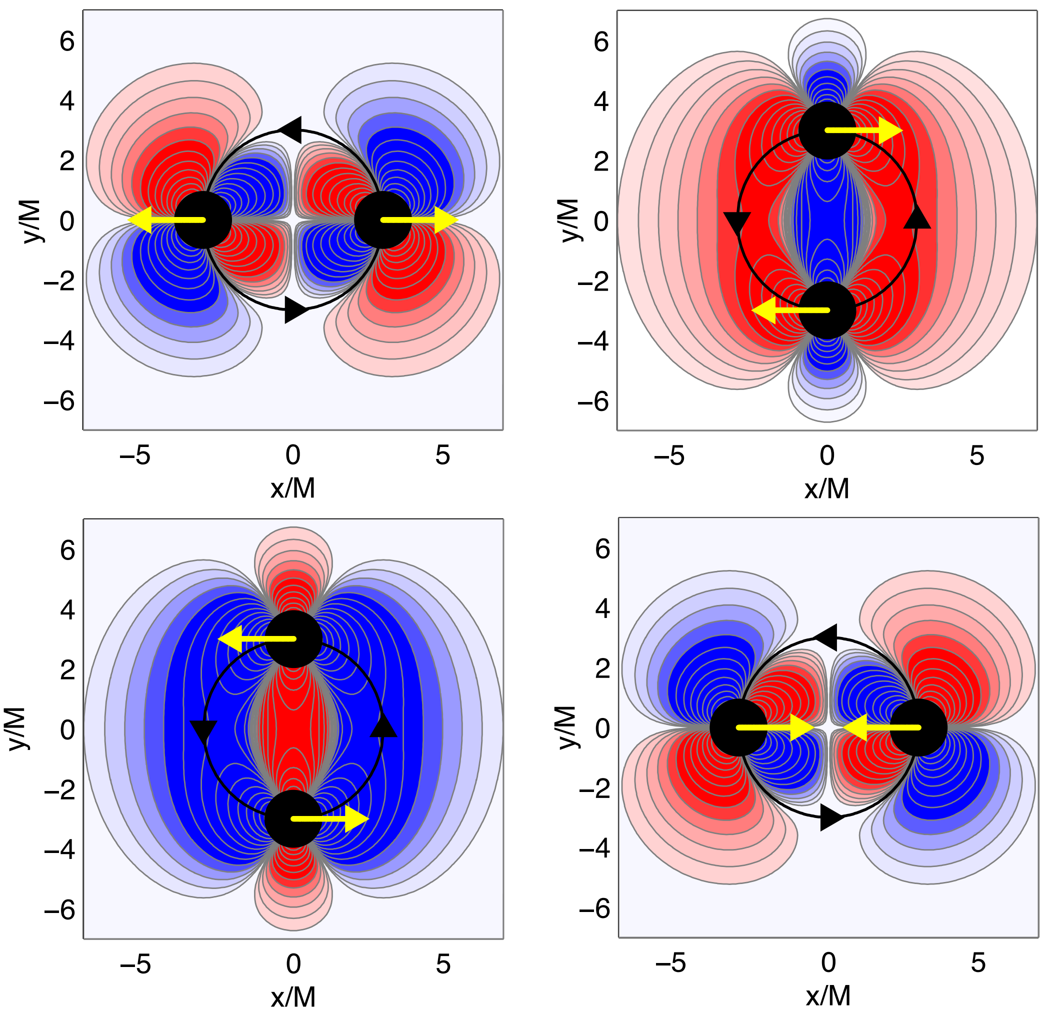


Figure 13.5: Field Momentum Density

The four pictures show the $z$-component of field-momentum density $\delta\tau^{0z}$ in the orbital plane at four different times, a quarter orbit apart. Red represents positive momentum density (coming out of the paper), and blue, negative (going into the paper). Only the piece of momentum density $\delta\tau^{0z}$ that flows during bobbing (equation (13.15)) is depicted. The yellow arrows are the black holes' vectorial spins; the large, black arrowed circle shows the orbital path of the two holes. In the top left picture, one sees the density of momentum when the black holes are at the top of their bob (maximum $z$) and momentarily stationary. The gravitational-field momentum is zero, but the momentum density itself shows rich structure. A quarter orbit later, in the top right, the holes are moving downward (into the paper) at top speed. The momentum between the black holes (blue region) flows into the paper with them, while surrounding momentum (red region) flows out of the paper ($+z$-direction). A half orbit after the first picture, in the lower left, the holes are momentarily at rest at the bottom of their bob (minimum $z$), the net field momentum is zero, and the momentum distribution is opposite that in the first picture (as one would expect during sinusoidal bobbing). Similarly, three quarters of the way through the orbit, in the lower right, the holes have reached their maximum upward speed, and the momentum distribution is identical to the second picture, but with the opposite sign.

relativity (e.g., Box 5.6 of MTW [1]), we define the star's center-of-mass world line to be that set of events $x^\mu_{\rm cm}$ satisfying the covariant field-theory-in-flat-spacetime relationship

$$S^{\alpha\beta}p_\beta = 0 \; . \tag{13.22}$$

Here $p^\beta = \int \tau^{0\beta} d^3x$ is the body's 4-momentum and

$$S^{\alpha\beta} \equiv \int [(x^\alpha - x^\alpha_{\rm cm})\tau^{\beta 0} - (x^\beta - x^\beta_{\rm cm})\tau^{\alpha 0}] d^3x \tag{13.23}$$

is the body's tensorial angular momentum. Here the integrals extend over the star's interior, and because the star's momentum is changing, we take the time component of $x^\mu_{\rm cm}$ to be the same as the time at which the integral is performed, $x^0_{\rm cm} = x^0$. (If the momentum were not changing, this restriction would be unnecessary; cf. Box 5.6 of MTW.)

In a reference frame where the body moves with ordinary velocity $v^j = p^j/p^0$, equation (13.22) says $S^{i0} = S^{ij}v_j$. We wish to rewrite this in a more illuminating form, accurate to first order in the velocity $\boldsymbol{v}$. At that accuracy, we can evaluate $S^{ij}$ in the body's rest frame, obtaining $S^{ij} = \epsilon^{ijk}S_k$ where $S_k$ is the body's spin angular momentum

$$S_k = \int \epsilon_{klm}(x^l - x^l_{\rm cm})\tau^{m0} d^3x \; . \tag{13.24}$$

Using definition (13.23) of $S^{i0}$ with $x^0_{\rm cm} = x^0$, our definition (13.22) of the center of mass then takes the concrete form

$$m\boldsymbol{x}_{\rm cm} = \int \boldsymbol{x}\tau^{00} d^3x - \boldsymbol{v} \times \boldsymbol{S} \; . \tag{13.25}$$

Here on the left side we have replaced $p^0 = \int \tau^{00} d^3x$ by its value in the body's rest frame, which is the mass $m$, since the two differ by amounts quadratic in $\boldsymbol{v}$.

Notice that, *when computed in the body's rest frame so* $\boldsymbol{v} = 0$*, the center of mass is* $m\boldsymbol{x}_{\rm cm} = \int \boldsymbol{x}\tau^{00} d^3x$*, but when computed in any frame moving slowly with respect to the rest frame, this expression must be corrected by the term* $-\boldsymbol{v} \times \boldsymbol{S}$*.* This is called the *physical spin supplementary* *condition* [162].

In our Harmonic coordinate system and at the 1.5PN order of our analysis, the dominant, time-time component of the EFEs (13.3) reduces to $\eta^{\mu\nu}\mathfrak{g}^{00}{}_{,\mu\nu} = 16\pi\tau^{00}$. The type of analysis carried out in section 19.1 of MTW [1] then reveals that *in the star's rest frame, the monopolar part of its* $\mathfrak{g}^{00}$ *is centered on the location* $\boldsymbol{x}_{\rm cm}$*; or, equivalently, when one expands the star's* $\mathfrak{g}^{00}$ *around* $\boldsymbol{x}_{\rm cm}$ *in its own rest frame, there is no dipolar* $1/r^2$ *term (no mass dipole moment). This well-known result (e.g., [163, 164]) can be used as an alternative definition of* $\boldsymbol{x}_{\rm cm}$*—a definition that works for black holes as well as for stars.*

Using this monopolar-field-centered definition of $\boldsymbol{x}_{\rm cm}$, Thorne and Hartle [164] have employed matched asymptotic expansions (valid for black holes) to derive the equations of motion for a system of compact bodies (e.g., a compact binary) (their equations (4.10) and (4.11)). For a compact binary, the spin-induced contributions to these equations of motion at 1.5PN order are (equation (4.11c) of Thorne and Hartle)

$$\begin{aligned} m_A \frac{d\delta \boldsymbol{v}_A}{dt} &= \frac{m_A}{r_{AB}^3}\left[6\boldsymbol{n}_{AB}(\boldsymbol{S}_B \times \boldsymbol{n}_{AB}\cdot \boldsymbol{v}_{AB}) + 4\boldsymbol{S}_B \times \boldsymbol{v}_{AB}\right. \\ &\quad \left. -6(\boldsymbol{S}_B \times \boldsymbol{n}_{AB})(\boldsymbol{v}_{AB}\cdot \boldsymbol{n}_{AB})\right] \\ &\quad +\frac{m_B}{r_{AB}^3}\left[6\boldsymbol{n}_{AB}(\boldsymbol{S}_A \times \boldsymbol{n}_{AB}\cdot \boldsymbol{v}_{AB}) + 3\boldsymbol{S}_A \times \boldsymbol{v}_{AB}\right. \\ &\quad \left. -3(\boldsymbol{S}_A \times \boldsymbol{n}_{AB})(\boldsymbol{v}_{AB}\cdot \boldsymbol{n}_{AB})\right] \,. \end{aligned} \tag{13.26}$$

Here

$$\boldsymbol{v}_A \equiv \frac{d\boldsymbol{x}_{{\rm cm}\,A}}{dt}\,, \quad \delta\boldsymbol{v}_A = \frac{d\delta\boldsymbol{x}_{{\rm cm}\,A}}{dt}\,, \quad \boldsymbol{v}_{AB} = \boldsymbol{v}_A - \boldsymbol{v}_B \tag{13.27}$$

are the velocity of (the center of mass of) body $A$, the spin-induced perturbation of that velocity, and the relative velocity of bodies $A$ and $B$. The first two lines of equation (13.26) are due to frame dragging by the other body (body $B$); the last two lines are a force due to the coupling of body $A$'s spin to $B$'s spacetime curvature.

#### 13.3.2.1 Equations of Motion Specialized to the Extreme-Kick Configuration

As in the previous section, we now specialize the above discussion to the extreme-kick configuration. In this configuration we are trying to explain the bobbing motion of the bodies as they orbit each other (i.e., the motion of the bodies perpendicular to the standard orbital plane). As noted above for the equal mass case, the symmetries of this configuration are such that $\boldsymbol{v}_A = -\boldsymbol{v}_B$, $\boldsymbol{S}_A = -\boldsymbol{S}_B$, and $\boldsymbol{v}_{AB} \cdot \boldsymbol{n}_{AB} = 0$. Since we are only interested in the portion of the equations of motion perpendicular to the orbital plane, the necessary portions of the equations of motion we shall look at are:

$$\left(\frac{d^2\delta\boldsymbol{x}_{\mathrm{cm}\,A}}{dt^2}\right)_{\mathrm{FD}} = \frac{1}{r_{AB}^3} 4\boldsymbol{S}_B \times \boldsymbol{v}_{AB} \ , \qquad (13.28a)$$

$$\left(\frac{d^2\delta\boldsymbol{x}_{\mathrm{cm}\,A}}{dt^2}\right)_{\mathrm{SC}} = \frac{1}{r_{AB}^3} 3\boldsymbol{S}_A \times \boldsymbol{v}_{AB} \ , \qquad (13.28b)$$

where the subscript FD refers to the frame dragging piece, while the subscript SC refers to the spin-curvature coupling piece. The sum of these two effects gives

$$\left(\frac{d^2\delta\boldsymbol{x}_A}{dt^2}\right)_{\text{spin effects}} = -\frac{2}{r_{AB}^3}\boldsymbol{S}_A \times \boldsymbol{v}_A \ , \qquad (13.29)$$

where we have used the fact that $\boldsymbol{S}_A = -\boldsymbol{S}_B$ and $\boldsymbol{v}_{AB} = \boldsymbol{v}_A - \boldsymbol{v}_B = 2\boldsymbol{v}_A$. We get the same acceleration of hole $B$ by replacing all subscript $A$'s by subscript $B$'s because $\boldsymbol{S}_B = -\boldsymbol{S}_A$, $\boldsymbol{v}_B = -\boldsymbol{v}_A$.

We can easily integrate this equation in time by noting that the spin precesses much more slowly than the orbital motion so $\boldsymbol{S}_A$ can be approximated as constant, and noting that $\boldsymbol{v}_A$ rotates with angular velocity $\Omega = \sqrt{M/r_{AB}^3} = \sqrt{2m/r_{AB}^3}$, where $M$ is the total mass and $m$ is the mass of each hole. The result, after one integration, can be written as

$$m\delta\boldsymbol{v}_A = m\delta\boldsymbol{v}_B = -\frac{m}{r_{AB}^2}\boldsymbol{S}_A \times \boldsymbol{n}_{AB} \ . \qquad (13.30)$$

These pieces of the total momentum we will call the *kinetic* momentum.

### 13.3.3 The Momenta of the Binary's Bodies

Let us now turn our attention to the total momentum contained by the bodies. This is done for two cases, first for stars where we can integrate over the interior, and then for black holes where we must convert the volume integrals to surface integrals. We shall find that both methods yield the same result. We initially omit the star's label $A$ or $B$ for ease of notation.

#### 13.3.3.1 The Momentum of a Star

For a star we can derive an expression for the momentum $p^j = \int \tau^{0j} d^3x$ (with the integral over the star's interior) in terms of the star's velocity $v^j = dx^j_{\rm cm}/dt$ by differentiating the center-of-mass equation (13.25) with respect to time. To allow for the possibility that the mass might change with time, we set $m = \int \tau^{00} d^3x$ before doing the differentiation; i.e., we differentiate

$$\boldsymbol{x}_{\rm cm} \int_A \tau^{00} d^3x = \int_A \boldsymbol{x} \tau^{00} d^3x - \boldsymbol{v} \times \boldsymbol{S} \ . \tag{13.31}$$

Using $\tau^{00}{}_{,0} = -\tau^{0k}{}_{,k}$ and Gauss's theorem, we bring the left side into the form $\boldsymbol{v} \int_A \tau_{00} d^3x - \boldsymbol{x}_{\rm cm} \int_{\partial A} (\tau^{0j} - \tau^{00} v^j) d\Sigma_j$. The last term arises from the motion of the surface of the star through space with velocity $\boldsymbol{v}$. Manipulating the time derivative of the integral on the right side of equation (13.31) in this same way, we bring it into the form $\int_A \tau^{0j} d^3x - \int_{\partial A} x^j (\tau^{0k} - \tau^{00} v^k) d\Sigma_k = p^j - \int_{\partial A} x^j (\tau^{0k} - \tau^{00} v^k) d\Sigma_k$, where $p^j$ is the star's momentum. Inserting these expressions for the left side and the right-side integral into equation (13.31), noting that the star's spin angular momentum evolves (due to precession) far more slowly than its velocity, denoting the time derivative of its velocity by $d\boldsymbol{v}/dt = \boldsymbol{a}$ (acceleration), solving for $\boldsymbol{p}$, and restoring subscript $A$s, we obtain

$$\boldsymbol{p}_A = m_A \boldsymbol{v}_A + \int_{\partial A} (\boldsymbol{x} - \boldsymbol{x}_{{\rm cm}\, A})(\tau^{0k} - \tau^{00} v^k_A) d\Sigma_k + \boldsymbol{a}_A \times \boldsymbol{S}_A \ . \tag{13.32}$$

Although we have derived this equation for a star, it must be true also for a black hole. The reason is that all the quantities that appear in it are definable without any need for integrating over the body's interior, and all are expressible in terms of the binary's masses and spins and its bodies' vectorial separation, in manners that are insensitive to whether the bodies are stars or holes. To illustrate this statement, in section 13.3.3.2 we deduce (13.32) for a black hole, restricting ourselves to spin-induced portion of the momentum that is being exchanged with the field, $\delta \boldsymbol{p}_A$.

It is this $\delta \boldsymbol{p}_A$ that interests us. Because the spin has no influence on $\tau^{00}$ at the relevant order (which is $\delta\tau^{0k} \sim gH$ and $\delta\tau^{00} \sim g^2$ where $g$ and $H$ are the gravitoelectric and gravitomagnetic fields), equation (13.32) implies that

$$\delta \boldsymbol{p}_A = m_A \delta \boldsymbol{v}_A + \int_{\partial A} (\boldsymbol{x} - \boldsymbol{x}_{\mathrm{cm}\,A}) \delta\tau^{0k} d\Sigma_k + \boldsymbol{a}_A \times \boldsymbol{S}_A \; . \tag{13.33}$$

The acceleration $\boldsymbol{a}_A$ of body $A$ is, at the order needed, just the gravitoelectric field of body $B$ at the location of $A$, $\boldsymbol{a}_A = -(m_B/r_{AB}^2)\boldsymbol{n}_{AB}$. Performing the surface integral on a sphere just above the body's physical surface we can write $\boldsymbol{x} - \boldsymbol{x}_{\mathrm{cm}\,A} = \boldsymbol{n}_A r_A$ and $d\Sigma_k = r_A^2 n_A^k d\Omega_A$. Inserting these into equation (13.33), we obtain

$$\delta \boldsymbol{p}_A = \underbrace{m_A \delta \boldsymbol{v}_A}_{\substack{\text{kinetic}\\ \text{term}}} + \underbrace{\int_{\partial A} r_A^3 \delta\tau^{0k} \boldsymbol{n}_A n_A^k d\Omega_A}_{\text{surface term}} + \underbrace{\frac{m_B}{r_{AB}^2} \boldsymbol{S}_A \times \boldsymbol{n}_{AB}}_{\text{SSC term}} \; . \tag{13.34}$$

Here "SSC term" refers to the "spin supplementary condition" required to get the correct, physical center of mass; see text following equation (13.25). In the surface term, the field momentum density $\delta\tau^{0k}$ is given by equation (13.17). The second term ($A \leftrightarrow B$) is smaller than the first by $M/r_{AB}$ and thus is negligible. Inserting the first term into the integral, using $(1/r_A)_{,qp} = (3n_A^q n_A^p - \delta_{qp})/r_A^3$ and $(1/r_B)_{,l} = -n_B^l/r_B^2$, and $\int n_A^j n_A^l d\Omega_A = \frac{4\pi}{3}\delta_{jl}$, we bring equation (13.34) into the form

$$\begin{aligned} \delta \boldsymbol{p}_A &= \underbrace{m_A \delta \boldsymbol{v}_A}_{\substack{\text{kinetic}\\ \text{term}}} \underbrace{- \frac{2}{3} \frac{m_B}{r_{AB}^2} \boldsymbol{S}_A \times \boldsymbol{n}_{AB}}_{\text{surface term}} + \underbrace{\frac{m_B}{r_{AB}^2} \boldsymbol{S}_A \times \boldsymbol{n}_{AB}}_{\text{SSC term}} \\ &= m_A \delta \boldsymbol{v}_A + \frac{1}{3} \frac{m_B}{r_{AB}^2} \boldsymbol{S}_A \times \boldsymbol{n}_{AB} \; . \end{aligned} \tag{13.35}$$

#### 13.3.3.2 The Momentum of a Black Hole

In section 13.3.3.1 we derived expression (13.32) for the momentum of a body in a binary, assuming the body is a star so we could do volume integrals, and we then asserted that this expression is also valid for black holes. The spin-induced portion of this expression that gets exchanged with the field as the body moves is given by equation (13.33), which reduces to (13.35). In this section we shall sketch a derivation of equation (13.35) directly from the surface-integral definition (13.8b) of a black hole's momentum,

$$\delta p_A^j = \frac{1}{16\pi}\int_{\partial A} \delta H^{j\alpha 0k}{}_{,\alpha} d\Sigma_k \ . \tag{13.36}$$

To evaluate this surface integral up to desired 1.5PN-order accuracy turns out to require some 2.5PN fields. Qualitatively, this can be anticipated because the superpotential we use in the surface integral is *sourced* by the spin-orbit piece of field momentum, and therefore necessarily a nonleading PN term. One can see this more clearly by expanding $\delta H^{j\alpha 0k}{}_{,\alpha}$ in terms of the metric density and using the symmetries of the superpotential $H$ (which are the same as the Riemann tensor). In general, the momentum is given by

$$\delta p_A^j = -\frac{1}{16\pi}\int_{\partial A} (\mathfrak{g}^{jk}\mathfrak{g}^{\alpha 0} - \mathfrak{g}^{j\alpha}\mathfrak{g}^{0k})_{,\alpha} d\Sigma_k \ . \tag{13.37}$$

In Harmonic gauge, however, $\mathfrak{g}^{\alpha\beta}{}_{,\beta} = 0$, and the spatial metric is flat until 2PN order while the time-space components are of 1.5PN order. As a result, the terms at lowest and next-to-lowest PN order are contained within two terms,

$$\delta p_A^j = \frac{1}{16\pi}\int_{\partial A} (\mathfrak{g}^{j0}{}_{,k} + \mathfrak{g}^{jk}{}_{,0}) d\Sigma_k \ . \tag{13.38}$$

In this expression, the momentum arises from linear terms involving the metric density, instead of quadratic ones. As a result, one must keep pieces of the metric perturbation that are of higher PN accuracy. (Note: if we were to evaluate the time derivative of $\delta \boldsymbol{p}_A$ using the surface integral (13.9), we would not face such a delicacy; the integrand there is quadratic and requires only 1.5PN fields for its evaluation.)

To find the momentum in terms of the standard post-Newtonian parameters, we resort to a standard way that the metric perturbations are written in recent post-Newtonian literature, e.g., by Blanchet, Faye, and Ponsot [165]:

$$
\begin{aligned}
g_{00} &= -1 + 2V - 2V^2 + 8\hat{X} \ , && (13.39a) \\
g_{i0} &= -4V_i - 8\hat{R}_i \ , && (13.39b) \\
g_{ij} &= \delta_{ij}(1 + 2V + 2V^2) + 4\hat{W}_{ij} \ , && (13.39c) \\
\sqrt{-g} &= 1 + 2V + 4V^2 + 2\hat{W}_{kk} \ . && (13.39d)
\end{aligned}
$$

For spinning systems, we adopt the notation of Tagoshi, Ohashi, and Owen [166] where $\mathcal{O}(m,n)$ means to order $c^m$ for nonspinning terms and $\chi c^n$ for terms involving a single spin $\chi$. (Here $\chi = |\boldsymbol{S}|/m^2$ is the body's dimensionless spin.) In this notation, terms we are interested in are of the order $\mathcal{O}(3,6)$, while the above post-Newtonian potentials have been obtained up to the following orders [166, 167]:

$$
\begin{aligned}
&V = \mathcal{O}(2,5), \quad V_j = \mathcal{O}(3,4), \\
&\hat{W}_{jk} = \mathcal{O}(4,5), \quad \hat{R}_j = \mathcal{O}(5,6). && (13.40)
\end{aligned}
$$

In terms of these post-Newtonian potentials, $V$, $V_i$, $\hat{R}_i$, $\hat{X}$ and $\hat{W}_{ij}$, the perturbed metric density is

$$
\begin{aligned}
\mathfrak{g}^{00} &= -1 - 4V - 2\left(\hat{W}_{kk} + 4V^2\right) + \mathcal{O}(6,7), && (13.41a) \\
\mathfrak{g}^{0i} &= -4V_i - 8\left(\hat{R}_i + VV_i\right) + \mathcal{O}(6,7), && (13.41b) \\
\mathfrak{g}^{ij} &= \delta_{ij} - 4\left(\hat{W}_{ij} - \frac{1}{2}\delta_{ij}\hat{W}_{kk}\right) + \mathcal{O}(6,7). && (13.41c)
\end{aligned}
$$

As a consequence, equation (13.38) is given by

$$\delta p^j_A = \frac{1}{16\pi}\int_{\partial A}\left\{\left[-4V_j - 8\left(\hat{R}_{j(S)} + V_{(m)}V_{j(S)}\right)\right]_{,k} -4\left[\hat{W}_{jk(S)} - \frac{1}{2}\delta_{jk}\hat{W}_{ii(S)}\right]_{,0}\right\}d\Sigma_k\,, \tag{13.42}$$

where a subscript $(S)$ means keep only the parts of those potentials proportional to the spins of the bodies, and a subscript $(M)$ involves monopolar pieces of the potential without spins (proportional to the masses of the bodies). Terms without a subscript have both pieces.

Tagoshi, Ohashi and Owen express the potentials $V_{(M)}$, $V_j$, $\hat{R}_{j(S)}$ and $\hat{W}_{jk(S)}$ in terms of the bodies' masses, vectorial velocities, vectorial spins, and vectorial separations, and distance to the field-point location (their equations (A1a), (A1d), (A1f), and (A1g)). While the full equations are quite lengthy, the portions that generate momentum flow—those involving the coupling of the mass of one body to the spin of the other—are somewhat simpler. For convenience, we give these portions of the equations below, rewritten in our notation, with the typos noted by Faye, Blanchet, and Bounanno [167] corrected:

$$V_{(M)} = \frac{m_A}{r_A} + (A \leftrightarrow B)\,, \tag{13.43a}$$

$$V_j = \frac{m_A v^j_A}{r_A} + \epsilon_{jkl}S^k_A\left\{n^l_A\left[-\frac{3m_B}{2r^2_A r_{AB}} - \frac{m_B(\boldsymbol{n}_A\cdot\boldsymbol{n}_{AB})}{4r_A r^2_{AB}}\right] + n^l_{AB}\frac{3m_B}{4r_A r_{AB}}\right\} +(A \leftrightarrow B)\,, \tag{13.43b}$$

$$\hat{W}_{jk(S)} = \frac{n^i_A}{r^2_A}\left[\frac{1}{2}\left(\epsilon_{ijl}S^l_A v^k_A + \epsilon_{ikl}S^l_A v^j_A\right) - \delta_{jk}\epsilon_{ilm}v^l_A S^m_A\right] + (A \leftrightarrow B)\,, \tag{13.43c}$$

$$\begin{aligned}\hat{R}_{j(S)} = {}& \epsilon_{jkl}S^k_A\left[n^l_A\left(-\frac{m_B}{2r^2_A r_{AB}} + \frac{m_B}{r_{AB}s^2}\right) + n^l_{AB}\left(-\frac{m_B}{2r_A r^2_{AB}} + \frac{m_B}{2r^2_{AB}r_B} + \frac{m_B}{r_A s^2}\right)\right. \\ & \left. +n^l_B\left(\frac{m_B}{r_A s^2} + \frac{m_B}{r_{AB}s^2}\right)\right] \\ & +n^j_A\epsilon_{ikl}S^l_A\left[n^i_A(n^k_{AB}+n^k_B)\left(\frac{m_B}{r_A s^2} + \frac{2m_B}{s^3}\right) - 2n^i_{AB}n^k_B\frac{m_B}{s^3}\right] \\ & +n^j_{AB}\epsilon_{ikl}S^l_A\left[-2n^i_A n^k_b\frac{m_B}{s^3} + (n^i_A + n^i_B)n^k_{AB}\left(-\frac{m_B}{r_{AB}s^2} - \frac{2m_B}{s^3}\right)\right] \\ & +(A \leftrightarrow B)\,.\end{aligned} \tag{13.43d}$$

Here, as before, $m_A$, $\boldsymbol{v}_A$, and $\boldsymbol{S}_A$ are the mass, velocity, and spin angular-momentum of object $A$; $r_A$ is the separation of body $A$ from a point in space and $r_{AB}$ is the separation of the two objects; and $\boldsymbol{n}_A$ and $\boldsymbol{n}_{AB}$ are unit vectors pointing along $r_A$ and $r_{AB}$, respectively. A new quantity, $s = r_A + r_B + r_{AB}$, has been introduced, in addition. Inserting these expressions into equation (13.42) gives us $\delta H^{j\alpha 0k}{}_{,\alpha}$, and the momentum of body $A$ is then found by performing a surface integral over $A$'s surface. The surface integrals are computed under the same assumptions as in section 13.3.1; namely the separation of the bodies is much larger than their radii, and each surface of integration is a sphere immediately above a body's surface. When they are computed, they give the same result as equation (13.35),

$$\delta \boldsymbol{p}_A = m_A \delta \boldsymbol{v}_A + \frac{1}{3}\frac{m_B}{r_{AB}^2} \boldsymbol{S}_A \times \boldsymbol{n}_{AB} \ . \tag{13.44}$$

As before, the momentum for body $B$ is given by exchanging $A$ and $B$.

As a consistency check, we can evaluate the system's total momentum by doing a surface integral at infinity:

$$\delta p^j_{\rm tot} = \frac{1}{16\pi} \oint_{\mathcal{S}} \delta H^{j\alpha 0k}{}_{,\alpha} d\Sigma_k \ . \tag{13.45}$$

The quantity $\delta H^{j\alpha 0k}{}_{,\alpha}$ is exactly the same as above, from which one can find

$$\delta \boldsymbol{p}_{\rm tot} = m_A \delta \boldsymbol{v}_A + \frac{m_B}{r_{AB}^2} \boldsymbol{S}_A \times \boldsymbol{n}_{AB} + (A \leftrightarrow B) \ . \tag{13.46}$$

This, combined with the fact that

$$\delta \boldsymbol{p}_{\rm tot} = \delta \boldsymbol{p}_A + \delta \boldsymbol{p}_B + \delta \boldsymbol{p}_{\rm field} \ , \tag{13.47}$$

as well as equation (13.44), gives

$$\delta \boldsymbol{p}_{\rm field} = \frac{2 m_B}{3 r_{AB}^2} \boldsymbol{S}_A \times \boldsymbol{n}_{AB} + (A \leftrightarrow B), \tag{13.48}$$

as found in section 13.3.1.

## 13.4 Momentum Conservation

The total spin-induced momentum perturbation, $\delta\boldsymbol{p}_{\rm tot} = \delta\boldsymbol{p}_A + \delta\boldsymbol{p}_B + \delta\boldsymbol{p}_{\rm field}$ (equations (13.35) and (13.20)) is

$$\delta\boldsymbol{p}_{\rm tot} = m_A\delta\boldsymbol{v}_A + m_B\delta\boldsymbol{v}_B + \frac{1}{r_{AB}^2}(m_B\boldsymbol{S}_A - m_A\boldsymbol{S}_B)\times\boldsymbol{n}_{AB}\ . \tag{13.49}$$

Momentum conservation requires that the time derivative of this $\delta\boldsymbol{p}_{\rm tot}$ vanish. The time derivative of the kinetic terms can be read off the equation of motion (13.26):

$$\begin{aligned} & m_A\frac{d\delta\boldsymbol{v}_A}{dt} + m_B\frac{d\delta\boldsymbol{v}_B}{dt} \\ & = -(m_B\boldsymbol{S}_A - m_A\boldsymbol{S}_B)\times[\boldsymbol{v}_{AB} - 3(\boldsymbol{n}_{AB}\cdot\boldsymbol{v}_{AB})\boldsymbol{n}_{AB}]\ . \end{aligned} \tag{13.50}$$

By inserting $\boldsymbol{n}_{AB} = (\boldsymbol{x}_{{\rm cm}\,A} - \boldsymbol{x}_{{\rm cm}\,B})/r_{AB}$ into the second term of equation (13.49) and differentiating with respect to time, we obtain the negative of expression (13.50). Therefore,

$$d\delta\boldsymbol{p}_{\rm tot}/dt = 0\ ; \tag{13.51}$$

i.e., as the binary's evolution drives spin-induced momentum back and forth between the bodies and the field, the total momentum remains conserved, as it must.

Interestingly, during the summation of momentum terms, one finds that the surface terms in $\delta\boldsymbol{p}_A + \delta\boldsymbol{p}_B$ have exactly cancelled the field momentum $\delta\boldsymbol{p}_{\rm field}$, leaving the total momentum as the sum of the bodies' kinetic term and their SSC term.

### 13.4.1 Momentum Conservation for Extreme-Kick Configuration

Let us examine in detail how momentum conservation is achieved in the presence of the bodies' bobbing. Our detailed analysis (above) breaks each object's momentum perturbation $\delta\boldsymbol{p}_{A,B}$ into three terms, the *kinetic momentum* $m\delta\boldsymbol{v}_{A,B}$, a term due to the *SSC*, and a *surface* integral term

Table 13.1: Pieces of Total Momentum

| Body | Kinetic | | SSC | Surface | Total |
|---|---|---|---|---|---|
| | Frame-Dragging | Spin-Curvature | | | |
| $\boldsymbol{p}_A$ | $-4\boldsymbol{a}_B \times \boldsymbol{S}_B$ | $3\boldsymbol{a}_A \times \boldsymbol{S}_A$ | $\boldsymbol{a}_A \times \boldsymbol{S}_A$ | $-\frac{2}{3}\boldsymbol{a}_A \times \boldsymbol{S}_A$ | $-\frac{2}{3}\boldsymbol{a}_A \times \boldsymbol{S}_A$ |
| $\boldsymbol{p}_B$ | $-4\boldsymbol{a}_A \times \boldsymbol{S}_A$ | $3\boldsymbol{a}_B \times \boldsymbol{S}_B$ | $\boldsymbol{a}_B \times \boldsymbol{S}_B$ | $-\frac{2}{3}\boldsymbol{a}_B \times \boldsymbol{S}_B$ | $-\frac{2}{3}\boldsymbol{a}_B \times \boldsymbol{S}_B$ |
| $\boldsymbol{p}_{\rm field}$ | $\frac{2}{3}(\boldsymbol{a}_A \times \boldsymbol{S}_A + \boldsymbol{a}_B \times \boldsymbol{S}_B)$ | | | | |

Spin-dependent, time-varying pieces of body and field momenta at 1.5PN order, for the extreme-kick binary (circular orbit with spins antialigned and in the orbital plane). The body momenta are broken down into kinetic, SSC and surface terms and are expressed in terms of the bodies' spins $\boldsymbol{S}_{A,B}$ and Newtonian-order gravitational accelerations $\boldsymbol{a}_{A,B} = -m_{B,A}\boldsymbol{n}_{AB,BA}/r_{AB}^2$. See equations ((13.26)) and ((13.35)) for a similar decomposition in a generic binary.

(see table 13.1). The total kinetic momentum

$$m\delta\boldsymbol{v}_A + m\delta\boldsymbol{v}_B = -\left(\boldsymbol{a}_A \times \boldsymbol{S}_A + \boldsymbol{a}_B \times \boldsymbol{S}_B\right) \neq 0 \ , \tag{13.52}$$

is not conserved because of the noncancellation between the frame-dragging and spin-curvature coupling terms. The total body momentum $\delta\boldsymbol{p}_A + \delta\boldsymbol{p}_B$ is not conserved either; it sums up to 2/3 the total kinetic momentum:

$$\delta\boldsymbol{p}_A + \delta\boldsymbol{p}_B = -\frac{2}{3}(\boldsymbol{a}_A \times \boldsymbol{S}_A + \boldsymbol{a}_B \times \boldsymbol{S}_B) \neq 0 \ , \tag{13.53}$$

To achieve momentum conservation, there is a nonzero spin-dependent total field momentum distributed outside of the bodies, with

$$\delta\boldsymbol{p}_{\rm field} = \frac{2}{3}(\boldsymbol{a}_A \times \boldsymbol{S}_A + \boldsymbol{a}_B \times \boldsymbol{S}_B) \ . \tag{13.54}$$

Note that this total external field momentum is only $-2/3$ the spin-dependent total kinetic momentum—instead of the $-1$ that one might have naively expected.

## 13.5 Summary

We have studied generic binary compact objects and mometum flow that occurs between the bodies and the surrounding spacetime using the Landau-Lifshitz formalism. In this analysis, we have found that the momentum of the absolute motion of the binary system is balanced by the momentum contained in the surrounding gravitational field. These results were also specialized to the interesting case of spinning black holes in the extreme-kick configuration. We think this formalism holds great promise for understanding the dynamics of compact objects and anticipate additional insights and intuition gained from applying this sort of analysis to other interacting black hole environments.